Electronic structure and chemical bonding of B_5^- and B_5 by photoelectron spectroscopy and *ab initio* calculations

Hua-Jin Zhai and Lai-Sheng Wang[a)]
Department of Physics, Washington State University, Richland, Washington 99352 and W. R. Wiley Environmental Molecular Sciences Laboratory, Pacific Northwest National Laboratory, Richland, Washington 99352

Anastassia N. Alexandrova and Alexander I. Boldyrev[b)]
Department of Chemistry and Biochemistry, Utah State University, Logan, Utah 84322-0300

(Received 12 March 2002; accepted 12 August 2002)

The electronic structure and chemical bonding of B_5^- and B_5 were investigated using anion photoelectron spectroscopy and *ab initio* calculations. Vibrationally resolved photoelectron spectra were obtained for B_5^- and were compared to theoretical calculations performed at various levels of theory. Extensive searches were carried out for the global minimum of B_5^-, which was found to have a planar C_{2v} structure with a closed-shell ground state ($^1A_1$). Excellent agreement was observed between *ab initio* detachment energies and the experimental spectra, firmly establishing the ground-state structures for both B_5^- and B_5. The chemical bonding in B_5^- was investigated and compared to that in Al_5^-. While both B_5^- and Al_5^- have a similar C_{2v} planar structure, their π-bonding orbitals are different. In Al_5^-, a π-bonding orbital was previously observed to delocalize over only the three central atoms in the C_{2v} ground-state structure, whereas a similar π orbital ($1b_1$) was found to completely delocalize over all five atoms in the C_{2v} B_5^-. This π bonding in B_5^- makes it more rigid towards butterfly out-of-plane distortions relative to Al_5^-. © *2002 American Institute of Physics.* [DOI: 10.1063/1.1511184]

I. INTRODUCTION

Boron possesses a diverse and complex range of chemistry.[1,2] Even in elementary form boron exhibits a variety of allotropic modifications. The structural unit that dominates the various allotropes of boron is the B_{12} icosahedron. There are other three-dimensional (3D) structures known for boron, such as the B_6 octaheron and the B_{12} cubooctahedron. Two-dimensional boron networks are also found in some metal borides, but in the very rich borohydride chemistry 3D structures are dominant. Hence it seems that 3D structures should be expected for pure boron clusters too. Yet quite to the contrary, planar or quasiplanar structures have been proposed for small boron clusters, according to *ab initio* calculations.[3–28] In spite of many mass-spectrometry-based experimental studies on small boron clusters during the past decade,[4,29–35] experimental information on the geometrical and electronic structures of boron clusters is limited. Detailed spectroscopic investigations would be desirable in gaining insight into the electronic structure and chemical bonding of these electron-deficient cluster species, as well as in testing the available theoretical calculations.

Our recent work has shown that photodetachment photoelectron spectroscopy (PES) combined with *ab initio* calculations provides a powerful means to obtain information about the structure and bonding of novel gaseous clusters.[36] In the current paper, we present a combined PES and *ab initio* study of the B_5^- and B_5 species. PES spectra were obtained at three photon energies (355, 266, and 193 nm) for B_5^-. Vibrationally resolved spectra were measured at the two lower detachment photon energies. Numerous PES features were observed and compared to the *ab initio* calculations. Extensive theoretical searches were performed for both B_5^- and B_5. The excellent agreement between the *ab initio* detachment energies of the C_{2v} global minimum of B_5^- and the experimental PES spectra firmly established the ground-state structures for both B_5^- and B_5. A molecular orbital analysis was carried out to investigate the detailed chemical bonding in B_5^- and compared to that in Al_5^-. The combined experimental and theoretical effort allowed us to fully characterize the structures and chemical bonding of B_5^- and B_5.

II. EXPERIMENTAL METHOD

The experiment was carried out using a magnetic-bottle time-of-flight PES apparatus equipped with a laser vaporization supersonic cluster source.[37,38] Briefly, the B_5^- anions were produced by laser vaporization of a pure boron target in the presence of a helium carrier gas. Various clusters were produced from the cluster source and were mass analyzed using a time-of-flight mass spectrometer. The B_5^- species were mass selected and decelerated before being photodetached. Three detachment photon energies were used in the current experiments: 355 nm (3.496 eV), 266 nm (4.661 eV), and 193 nm (6.424 eV). The photoelectron spectra were calibrated using the known spectrum of Rh^-, and the resolution of the apparatus was better than 30 meV for 1 eV electrons.

It should be pointed out that although it was not difficult to observe mass spectra with a wide size range of B_n^- clus-

a)Electronic mail: ls.wang@pnl.gov
b)Electronic mail: boldyrev@cc.usu.edu

ters by laser vaporization, it was rather challenging to obtain high-quality PES spectra, primarily due to the low photodetachment cross sections of these light clusters and the difficulty to obtain cold cluster anions. The key to the current progress was the use of a large waiting-room nozzle, which could more efficiently cool cluster anions.[37–39] The temperature effects were further controlled by tuning the firing timing of the vaporization laser relative to the carrier gas, and choosing the later part of the cluster beam for photodetachment.[40–43] These efforts have allowed us to obtain well-resolved PES data for a wide size range of B_n^- clusters at different photodetachment energies. In the current paper, we report the results for one of the smallest cluster species, B_5^-. We note that B_5^- is the smallest species that could be produced under our current cluster source conditions with abundance high enough to perform photodetachment experiments.

III. COMPUTATIONAL METHODS

We first optimized geometries of B_5^- and B_5 employing analytical gradients with the polarized split-valence basis sets (6-311+G*) (Refs. 44–46) with a hybrid method, which includes a mixture of Hartree-Fock exchange with density-functional exchange-correlation potentials (B3LYP).[47–49] In order to test the validity of the one-electron approximation, we optimized geometries and calculated frequencies using the multiconfigurational complete-active-space self-consistent field method (CASSCF) with eight active electrons for B_5^- and seven active electrons for the neutral species as well as eight active molecular orbitals in both cases [CASSCF(8,8)/6-311+G* for B_5^- and CASSCF(7,8)/6-311+G* for B_5]. Optimized geometries and harmonic frequencies were refined using the restricted coupled-cluster method including single and double excitations and with triple excitations treated noniteratively [RCCSD(T)] (Refs. 50–53) and the same basis sets. The MP2 and UCCSD(T) calculations were not performed because of high spin contamination in the UHF wave functions. Vertical detachment energies (VDE's) from the lowest-energy structure of B_5^- were calculated using the outer valence Green function (OVGF) method[54–58] incorporated in GAUSSIAN 98. A few lowest VDE's were also calculated at the RCCSD(T)/6-311+G(2df) level of theory.[51] The core electrons were kept frozen in treating the electron correlation at the OVGF and RCCSD(T) levels of theory. The B3LYP/6-311+G*, CASSCF(7,8)/6-311+G*, CASSCF(8,8)/6-311+G*, and ROVGF/6-311+G(2df) calculations were performed using the GAUSSIAN 98 program.[59] The RCCSD(T)/6-311+G* and RCCSD(T)/6-311+G(2df) calculations were performed using the MOLPRO 99 program.[60] Molecular orbitals (MO's) were calculated at the RHF/6-311+G* level of theory. All MO pictures were made using the MOLDEN 3.4 program.[61]

IV. EXPERIMENTAL RESULTS

The PES spectra of B_5^- are shown in Fig. 1 at three detachment photon energies. The higher photon energy (193 nm) used in the current work allowed high-binding-energy features to be observed, whereas the lower photon energies (355 nm and 266 nm) allowed the accessible electronic transitions to be better resolved. All the observed detachment transitions, labeled with letters in Fig. 1, were well defined and well resolved. The *X* and *A* bands were vibrationally resolved, as indicated by the vertical lines in Fig. 1. The PES spectra represent electronic transitions from the ground state of B_5^- to the ground and low-lying excited states of the neutral B_5. Overall, four major detachment bands (*X*, *A*, *B*, and *C*) were observed for B_5^-.

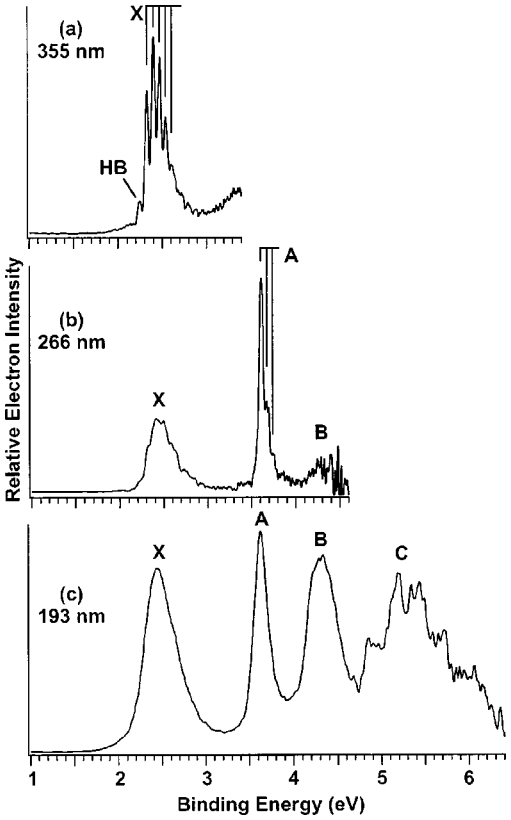

FIG. 1. Photoelectron spectra of B_5^- at (a) 355 nm (3.496 eV), (b) 266 nm (4.661 eV), and (c) 193 nm (6.424 eV). "HB" denotes a hot band transition.

The 355 nm spectrum [Fig. 1(a)] revealed a well-resolved vibrational progression for the ground-state transition with a 550 cm^{-1} spacing. The 0-0 transition defined an adiabatic detachment energy (ADE) of 2.33 eV for B_5^-, which also represents the adiabatic electron affinity (EA) of

TABLE I. Observed adiabatic and vertical electron binding energies (ADE's and VDE's), term values, and vibrational frequencies from the photoelectron spectra of B_5^-.

Observed feature	ADE (eV)[a]	VDE (eV)[a]	Term value (eV)	Vib. freq. (cm^{-1})[a,b]
X	2.33 (0.02)[c]	2.40 (0.02)	0	550 (40)
A	3.61 (0.02)	3.61 (0.02)	1.28	530 (50)
B	4.05 (0.05)	4.33 (0.05)	1.72	
C		4.7–6.2		

[a]The numbers in the parentheses represent the experimental uncertainty.
[b]The anion ground-state frequency was estimated to be 680 ± 60 cm^{-1} from the hot band transition (Fig. 1).
[c]The adiabatic electron affinity of B_5.

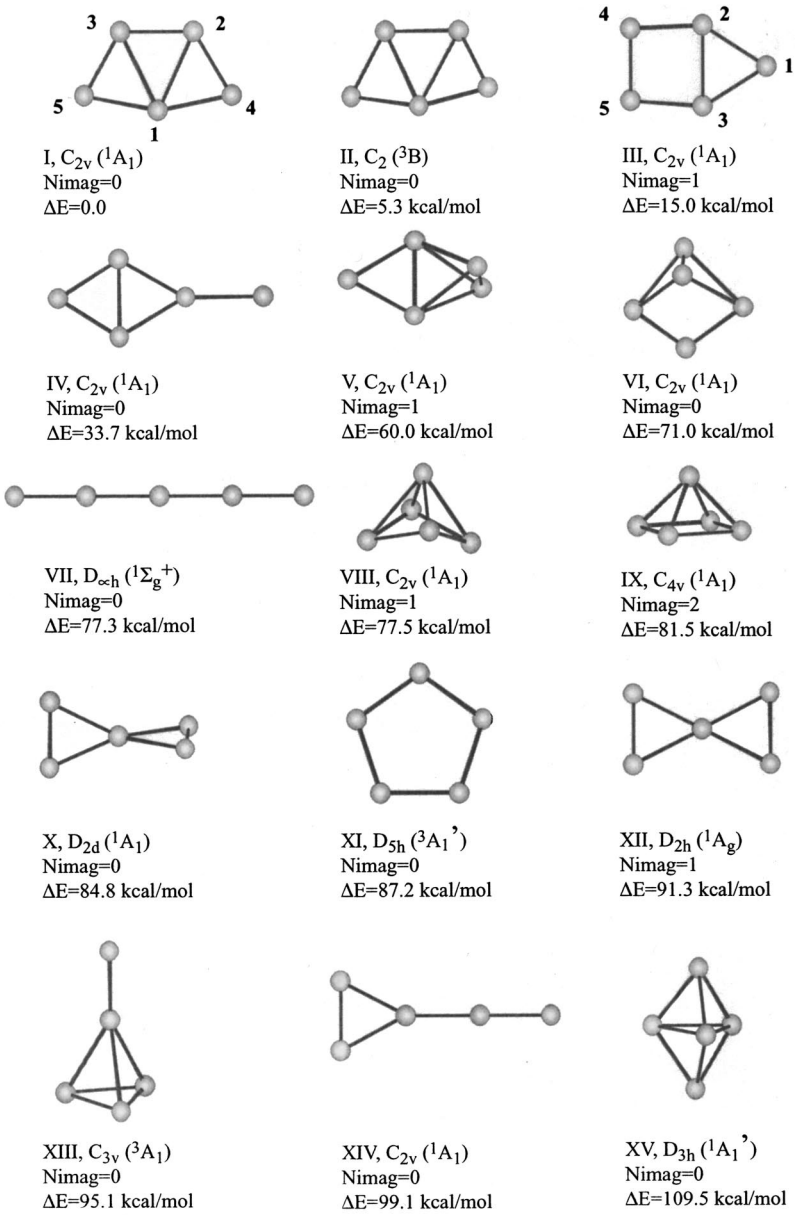

FIG. 2. Optimized structures of B_5^- at the B3LYP/6-311+G* level of theory.

the neutral B_5. The VDE was defined by the $1 \leftarrow 0$ transition at 2.40 eV. The weak feature at 2.24 eV, labeled as HB in Fig. 1(a), was assigned as a hot band transition, because the spacing between this feature and the 2.33 eV peak is much larger (680 cm^{-1}). The latter represents the vibrational frequency of the anion, indicating that a bonding electron was removed in the transition from the ground state of the anion to that of the neutral.

At 266 nm, a relatively sharp and intense band (*A*) was observed at 3.61 eV, as well as a weak feature (*B*) at higher binding energies. The *A* band displayed a short vibrational progression with an average spacing of 530 cm^{-1}, similar to that of the ground-state band (*X*). The *A* band represents the first excited state of B_5. The short vibrational progression suggests that there is little geometric change between the anion ground state and the first excited state of the neutral.

At 193 nm, the intensities of both the *X* and *B* bands were enhanced relative to the *A* band, which was dominant in the 266 nm spectrum. The *B* band was rather broad, but no vibrational progression was resolved, suggesting that more than one vibrational modes with low frequencies were likely to be active upon photodetachment. The VDE of feature *B* was measured from the band maximum to be 4.33 eV. The ADE was estimated from the threshold of band *B* to be 4.05 eV. The 193 nm spectrum also revealed congested features, broadly designated as the *C* band, at higher binding energies between 4.7 and 6.2 eV. Five fine features were discernible in this energy range. As will be shown from the theoretical results, there are two one-electron detachment channels with possibilities of multielectron transitions within this energy range. All the observed electron binding energies and spectroscopic constants for B_5 are summarized in Table I.

V. THEORETICAL RESULTS

First, we performed an extensive search for the most stable structures for B_5^- and B_5 using the B3LYP/6-311

TABLE II. Calculated molecular properties of structure I (Fig. 2) of B_5^-.

B_5^-, C_{2v}, $^1A_1$	B3LYP/ 6-311+G*	CASSCF(8,8)/ 6-311+G*	CCSD(T)/ 6-311+G*
E_{tot} (a.u.)	−124.080875	−123.252276	−123.677914
R(B1-B2,3) (Å)	1.738	1.752	1.765
R(B1-B4,5) (Å)	1.614	1.632	1.639
R(B2-B3) (Å)	1.577	1.557	1.607
R(B2-B4) (Å)	1.579	1.583	1.617
$\omega_1(a_1)$ (cm^{-1})	1259	1320	1196
$\omega_2(a_1)$ (cm^{-1})	965	985	928
$\omega_3(a_1)$ (cm^{-1})	719	738	710
$\omega_4(a_1)$ (cm^{-1})	638	647	593
$\omega_5(a_2)$ (cm^{-1})	374	402	357
$\omega_6(b_1)$ (cm^{-1})	253	277	202
$\omega_7(b_2)$ (cm^{-1})	1067	1121	1082
$\omega_8(b_2)$ (cm^{-1})	998	994	929
$\omega_9(b_2)$ (cm^{-1})	582	637	556

TABLE III. Calculated molecular properties of structure III (Fig. 2) of B_5^-.

B_5^-, C_{2v}, $^1A_1$	B3LYP/ 6-311+G*	CASSCF(8,8)/ 6-311+G*	RCCSD(T)/ 6-311+G*
E_{tot} (a.u.)	−124.056959	−123.242419	−123.65190[a]
R(B1-B2,3) (Å)	1.624	1.672	1.625
R(B2-B4) (Å)	1.579	1.576	1.579
R(B2-B3) (Å)	1.703	1.743	1.705
R(B4-B5) (Å)	1.539	1.557	1.540
$\omega_1(a_1)$ (cm^{-1})	1231	1224	1203
$\omega_2(a_1)$ (cm^{-1})	1060	1057	1019
$\omega_3(a_1)$ (cm^{-1})	931	877	908
$\omega_4(a_1)$ (cm^{-1})	714	695	699
$\omega_5(a_2)$ (cm^{-1})	254	301	104
$\omega_6(b_1)$ (cm^{-1})	212	276	59*i*
$\omega_7(b_2)$ (cm^{-1})	1134	1110	1184
$\omega_8(b_2)$ (cm^{-1})	683	610	678
$\omega_9(b_2)$ (cm^{-1})	565*i*	422*i*	600*i*

[a]Geometry optimization along the imaginary $\omega_6(b_1)$ mode results in a slightly nonplanar first-order saddle point, which is just 0.5 kcal/mol lower in energy.

+G* level of theory. A selected set of the lowest-energy structures identified in our search is presented in Figs. 2 and 3 for B_5^- and B_5, respectively.

The global minimum for B_5^- was found to be a planar C_{2v} structure (I) with an electronic configuration $1a_1^2 1b_2^2 2a_1^2 3a_1^2 1b_1^2 2b_2^2 4a_1^2 3b_2^2 (^1A_1)$, similar to that for the valence isoelectronic cluster Al_5^-.[63] We found a C_2 isomer (II, ^3B) just 5.3 kcal/mol higher at B3LYP/6-311 +G*. Other tested structures were all found to be more than 10 kcal/mol higher in energy (Fig. 2). These results are different from Al_5^-, where an isomer similar to structure-III was found to be only 0.9 kcal/mol higher at B3LYP/6-311 +G*.[63] Moreover, when geometries of Al_5^- were optimized at the MP2/6-311+G* level of theory, structure III became the global minimum and structure I became a first-order saddle point, although both structures were found to be slightly nonplanar. Before going to theories higher than B3LYP/6-311+G* we tested the applicability of the one-electron approximation by optimizing geometries and calculating frequencies for two structures (I and III) at the CASSCF(8,8)/6-311+G* level of theory (see Tables II and III). For both structures we found that the wave functions have appreciable multiconfigurational characters. For the most stable structure I we found that even though the Hartree–Fock configuration is still dominant ($C_{HF}=0.892$), the second configuration ($1a_1^2 1b_2^2 2a_1^2 3a_1^2 1b_1^2 2b_2^2 4a_1^2 3b_2^0 1a_2^0 5a_1^2$) contributes substantially ($C_{14}=-0.349$, here and hereafter the C_i coefficient represents the contribution of the corresponding excited configuration to the CASSCF wave function) to the CASSCF(8,8)/6-311+G* wave function. For structure III, the Hartree–Fock configuration is clearly dominant ($C_{HF}=0.923$) with the second configuration contributing modestly ($C_{14}=-0.198$). In spite of the multiconfigurational character of the wave functions for the two structures of B_5^-, we believe the CCSD(T) method is still applicable here, and hence we further optimized geometries for structures I and III at the CCSD(T)/6-311+G* level of theory. Structure I was found to be planar and structure III was found to be slightly nonplanar, but still being a first-order saddle point for the in-plane intramolecular rearrangement (Tables II and III). We tested the relative energies of the three lowest-energy structures (I, II, and III) at the RCCSD(T)/6-311+G(2df) level of theory. Structure I was found still to be the most stable one with structures II and III being 11.7 and 15.0 kcal/mol higher, respectively. The VDE calculated for structure II was found to be 1.92 eV at the RCCSD(T)/6-311+G(2df) level of theory, which is substantially off the experimental value of 2.40 ± 0.02 eV, whereas the calculated VDE for structure I is in excellent agreement with the experimental value. On the basis of these results we concluded that structure I is the true global minimum for B_5^-.

The B_5^- anion is isoelectronic with the CAl_4 molecule, which has a tetrahedral global minimum with the carbon atom at the center.[62] We optimized a similar B_5^- tetrahedral structure and found that it is a local minimum at the B3LYP/6-311+G* and CCSD(T)/6-311+G* levels of theory. However, the relative energy was found to be very high for the tetrahedral structure of B_5^-: 133 kcal/mol (B3LYP/6-311+G*) and 130 kcal/mol (CCSD(T)/6-311 +G(2df)//CCSD(T)/6-311+G*). The reason why the B_5^- anion is not stable at the tetrahedral structure is because of the high negative charge on the central boron atom [$Q(B_c) = -2.25|e|$ at the NPA QCISD/6-311+G* level of theory]. Therefore, structure I, in which one pair of electrons was transferred from the central atom to the peripheral three-center boron-boron bond, is more stable.

The global minimum for the neutral B_5 was found to be a C_{2v} planar structure (XVI, $^2B_2$) at B3LYP/6-311+G* with an electronic configuration $1a_1^2 1b_2^2 2a_1^2 3a_1^2 1b_1^2 2b_2^2 4a_1^2 3b_2^1$ (Fig. 3). This structure is derived from the anion B_5^- global minimum by detaching an electron from its highest occupied molecular orbital (HOMO). We did not find any alternative low-lying structures for the neutral B_5 cluster. We repeated CASSCF(7,8)/6-311+G* calculations for structure XVI. As in B_5^-, the CASSCF(7,8) wave function of B_5 has an appreciable multiconfigurational character (major contributors are $C_{HF}=0.884$, $C_9=-0.267$, $C_{64}=+0.185$, and C_{15}

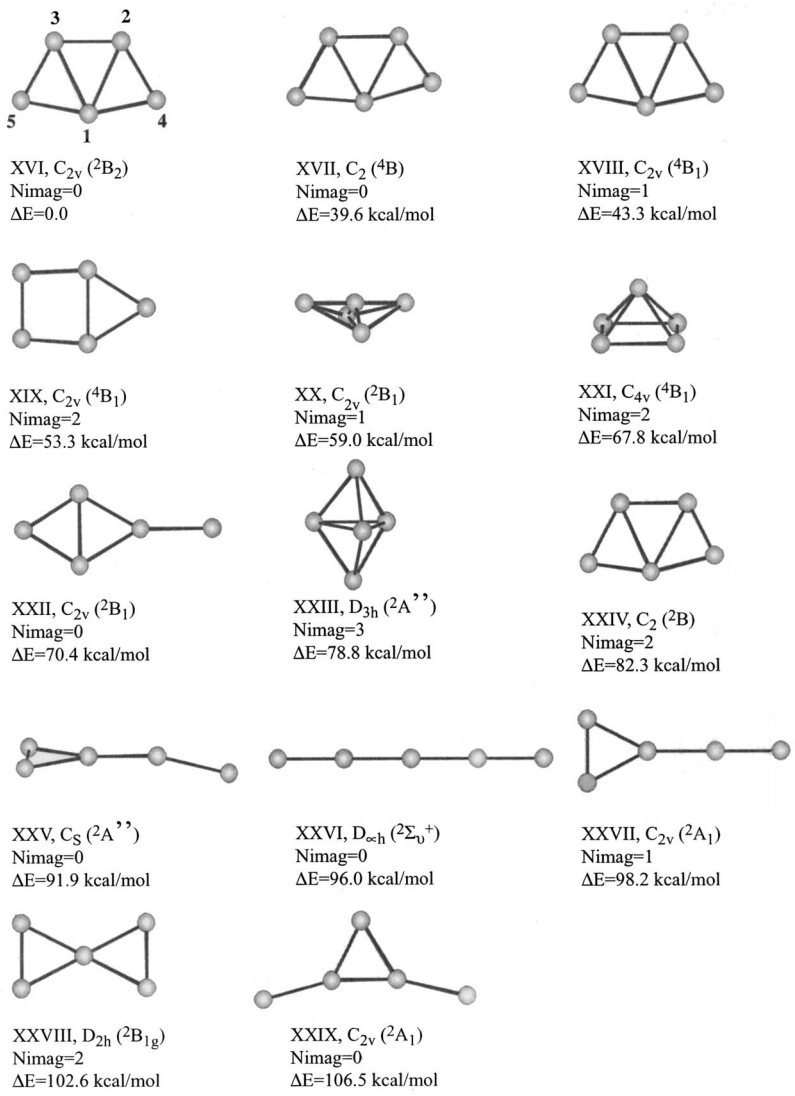

FIG. 3. Optimized structures of B_5 at the B3LYP/6-311+G* level of theory.

$=-0.154$). The multiconfigurational character of the B_5 wave function results in a high spin contamination in the UHF wave function. Therefore, CCSD(T) geometry optimization and frequency calculations were performed for B_5 at the RCCSD(T)/6-311+G* level of theory. Results at the B3LYP/6-311+G*, CASSCF(7,8)/6-311+G*, and RCCSD(T)/6-311+G* levels of theory were found to be in reasonable agreement with each other (Table IV).

VI. INTERPRETATION OF THE PES SPECTRA AND COMPARISON WITH THEORETICAL RESULTS

As shown in Sec. V, the global minimum of B_5^- was found to be the planar structure I (C_{2v}, $^1A_1$) with the electronic configuration $1a_1^2 1b_2^2 2a_1^2 3a_1^2 1b_1^2 2b_2^2 4a_1^2 3b_2^2$. As given in Table V, our calculated VDE for removal of an electron from the HOMO of the global minimum is 2.45 eV at the RCCSD(T)/6-311+G(2df) level of theory and 2.36 eV at the ROVGF/6-311+G(2df) level of theory. The pole strength was found to be 0.84, indicating that the detachment channel can be primarily described by a one-electron detachment process. These calculated numbers for the ground-state VDE are in excellent agreement with the measured VDE of 2.40 eV for this feature (Table I). The HOMO of B_5^- is a bonding orbital within the triangular wings B1-B2-B4 and B1-B3-B5 in the global minimum structure (Fig. 4). Detachment of an electron from this orbital should result in geom-

TABLE IV. Calculated molecular properties of the structure XVI (Fig. 3) of B_5.

B_5^-, C_{2v}, $^2B_2$	B3LYP/ 6-311+G*	CASSCF(7,8)/ 6-311+G*	RCCSD(T)/ 6-311+G*
E_{tot} (a.u.)	−124.003032	−123.218158	−123.596877
R(B1-B2,3) (Å)	1.835	1.868	1.870
R(B1-B4,5) (Å)	1.582	1.584	1.606
R(B2-B3) (Å)	1.553	1.552	1.584
R(B2-B4) (Å)	1.563	1.591	1.596
$\omega_1(a_1)$ (cm^{-1})	1332	1337	a
$\omega_2(a_1)$ (cm^{-1})	955	958	a
$\omega_3(a_1)$ (cm^{-1})	739	759	a
$\omega_4(a_1)$ (cm^{-1})	602	596	a
$\omega_5(a_2)$ (cm^{-1})	346	368	a
$\omega_6(b_1)$ (cm^{-1})	266	306	a
$\omega_7(b_2)$ (cm^{-1})	1159	1170	a
$\omega_8(b_2)$ (cm^{-1})	1024	939	a
$\omega_9(b_2)$ (cm^{-1})	478	527	a

[a]Frequencies have not been calculated at this level of theory.

TABLE V. Calculated one-electron detachment channels for the ground state of B_5^- (structure I).

Molecular orbital	VDE (theor.)[a] ROVGF/6-311+G(2df) (eV)	VDE (theor.) RCCSD(T)/6-311+G(2df) (eV)
$3b_2$	2.36 (0.84)	2.45
$4a_1$	4.00 (0.78)	3.75
$2b_2$	4.51 (0.86)	
$1b_1$	5.25 (0.87)	5.22
$3a_1$	5.78 (0.76)	

[a]The numbers in the parentheses indicate the pole strength, which characterizes the validity of the one-electron detachment picture.

etry relaxations within these wings. That is exactly what was found in B_5 upon geometry optimization (see data in Tables II and IV). The distances between atoms B1 and B2 (B3) became longer after electron detachment. Such geometry changes can be achieved through following the deformational normal mode $\omega_4(a_1)=596\ \mathrm{cm}^{-1}$ of the B_5 (Table IV). The experimentally measured vibrational frequency (550 cm^{-1}) is in excellent agreement with the calculated number. We thus assign the observed feature *X* (Fig. 1) straightforwardly to the transition from the anion ground state ($^1A_1$) to the neutral ground state ($^2B_2$), i.e., detachment of a $3b_2$ (HOMO) electron from the anion.

The excellent agreement for the ground-state transition between the theoretical and experimental results firmly established the identified ground state structures for both B_5^- and B_5. Hence, within the one-electron detachment picture, assignments of the higher PES features (Fig. 1) should be straightforward. Features *A* should be due to detachment from the HOMO-1 ($4a_1$). We note that the calculated VDE by ROVGF is off by ~0.4 eV compared to the experimental VDE (Table I). This is due to the multiconfigurational nature of this transition, as indicated by the low pole strength (0.78, Table V). However, excellent agreement was observed for this transition between the experimental VDE and the RCCSD(T)/6-311+G(2df) VDE (3.75 eV). Figure 4 shows that the $4a_1$ orbital is a strong bonding MO. However, the observed PES spectrum was relatively sharp with a very short vibrational progression. This suggests that the *A* state cannot be well described by the simple removal of an electron from the $4a_1$ orbital of B_5^-, consistent with the multiconfigurational nature of this transition.

Feature *B* at 4.33 eV (Table I) should correspond to removal of an electron from the HOMO-2 ($2b_2$). The calculated VDE at the ROVGF level is in good agreement with the experimental VDE, suggesting that this detachment channel can be well described by a one-electron process, consistent with the large pole strength. The broad width of this band was consistent with the strongly bonding nature of the $2b_2$ orbital. Because the symmetry of this state is the same as that of the ground state, we could not calculate its VDE at the CCSD(T) level of theory. However, as shown in Table V, when the pole strength of a detachment channel is large, i.e., for a primarily one-electron transition, the CCSD(T)

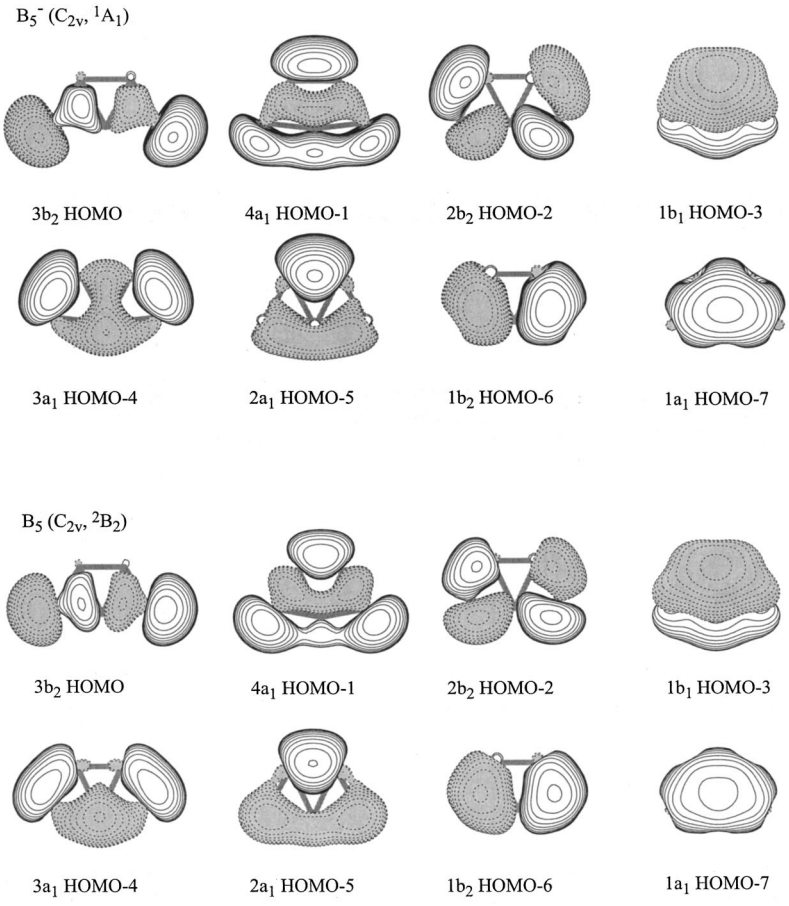

FIG. 4. Molecular orbital pictures for the C_{2v} global minima of B_5^- (structure I) and B_5 (structure XVI) (the order of the MO's according to the B_5^- OVGF calculations).

VDE is always within less than 0.1 eV of the ROVGF value.

The ROVGF VDE's for HOMO-3 and HOMO-4 are at 5.25 and 5.78 eV, which should contribute to the congested PES features observed between 4.7 and 6.2 eV. It should be stressed that at such high excitation energies many shake-up transitions may take place, contributing to the congested spectral features between 4.7 and 6.2 eV, because of the presence of many low-lying unoccupied MOs and the multiconfigurational nature of the ground states of B_5^- and B_5. Thus, a more quantitative interpretation of this part of the spectrum will need additional study using appropriate theoretical methods to treat shake-up processes and is beyond the focus of the current work.

VII. CHEMICAL BONDING IN B_5^- AND B_5

Chemical bonding in B_5^- and B_5 can be explained the same way as in Al_5^- and Al_5 because their occupied MOs are very similar (see Fig. 3 in Ref. 63), except that the smaller size of boron and the shorter B-B distances yield stronger bonding interactions within B_5^- and stronger MO overlaps. Molecular orbitals for B_5^- and B_5 look very similar (Fig. 4) and we will discuss only MO's in the anion. The peripheral four-center bond ($4a_1$, HOMO-1) contributes to the planarity of all four species. Both B_5^- and Al_5^- possess an out-of-plane π bond ($1b_1$, HOMO-3). However, there is a significant difference between these π MO's of B_5^- and Al_5^-. In Al_5^- the π MO was localized primarily on the three central Al atoms, making this cluster somewhat flexible in the area of the two wings. Indeed, at the B3LYP/6-311+G* level of theory, the normal mode $\omega_6(b_1)$ in Al_5^-, responsible for the butterfly out-of-plane vibrations, was found to be just 21 cm^{-1} and at the MP2/6-311+G* level that vibrational frequency became imaginary, leading to an out-of-planar distortion. The same π MO in B_5^- (HOMO-3, Fig. 4) is delocalized over all five boron atoms and that makes this cluster much more rigid towards the butterfly out-of-plane distortion: $\omega_6(b_1)=253\ cm^{-1}$ at B3LYP/6-311+G* and $\omega_6(b_1)=202\ cm^{-1}$ at CCSD(T)/6-311+G*. The complete delocalization of the π MO in B_5^- is intriguing, which is expected to contribute further to the planarity of B_5^- and B_5, in addition to the peripheral five-center bond. We will explore if that delocalization may contribute to the planarity of larger boron clusters in our future works.

VIII. CONCLUSIONS

Vibrationally resolved photoelectron spectra of the B_5^- clusters were obtained at three photon energies. Three well-resolved photodetachment features were observed at lower binding energies, whereas congested features were observed in the high-binding-energy regime. The electron affinity of B_5 was measured to be 2.33 ± 0.02 eV. An extensive search for the global minimum was performed for B_5^- and B_5 using the B3LYP/6-311+G* level of theory. The global minima for B_5^- and B_5 were both found to possess planar C_{2v} structures, similar to the most stable structures of Al_5^- and Al_5. The *ab initio* VDE's calculated from the lowest-energy structure of B_5^- was found to be in excellent agreement with the experimental ones for the three well-resolved lower-binding-energy PES features. The more congested spectral features above 4.7 eV were partially attributed to shake-up transitions as a result of multielectron transitions. Molecular orbital analyses for B_5^- revealed an interesting π MO, which was found to be completely delocalized over all five boron atoms. The delocalization of the π MO makes the planar B_5^- cluster much more rigid towards out-of-plane distortions compared to the Al_5^- cluster.

ACKNOWLEDGMENTS

The theoretical work done at Utah was supported by the donors of The Petroleum Research Fund (ACS-PRF Grant No. 35255-AC6), administered by the American Chemical Society. The experimental work done at Washington was supported by the National Science Foundation (Grant No. DMR-0095828) and performed at the W. R. Wiley Environmental Molecular Sciences Laboratory, a national scientific user facility sponsored by DOE Office of Biological and Environmental Research and located at Pacific Northwest National Laboratory, which is operated for the DOE by Battelle.

[1] F. A. Cotton, G. Wilkinson, C. A. Murillo, and M. Bochmann, *Advanced Inorganic Chemistry*, 6th ed. (Wiley, New York, 1999).
[2] N. N. Greenwood and A. Earnshaw, *Chemistry of Elements*, 2nd ed. (Butterworth-Heinemann, Oxford, 1997).
[3] A. C. Tang and Q. S. Li, Int. J. Quantum Chem. **29**, 579 (1986).
[4] L. Hanley, J. L. Whitten, and S. L. Anderson, J. Phys. Chem. **92**, 5803 (1988).
[5] R. Hernandez and J. Simons, J. Chem. Phys. **94**, 2961 (1991).
[6] A. U. Kato and E. Tanaka, J. Comput. Chem. **12**, 1097 (1991).
[7] H. Kato, K. Yamashita, and K. Morokuma, Chem. Phys. Lett. **190**, 361 (1992).
[8] J. M. L. Martin, J. P. Francois, and R. Gijbels, Chem. Phys. Lett. **189**, 529 (1992).
[9] R. Kawai and J. H. Weare, Chem. Phys. Lett. **191**, 311 (1992).
[10] A. K. Ray, I. A. Howard, and K. M. Kanal, Phys. Rev. B **45**, 14247 (1992).
[11] I. Boustani, Int. J. Quantum Chem. **52**, 1081 (1994).
[12] A. Meden, J. Mavri, M. Bele, and S. Pejovnik, J. Phys. Chem. **99**, 4252 (1995).
[13] I. Boustani, Chem. Phys. Lett. **233**, 273 (1995).
[14] I. Boustani, Chem. Phys. Lett. **240**, 135 (1995).
[15] I. Boustani, Surf. Sci. **370**, 355 (1996).
[16] A. Ricca and C. W. Bauschlicher, Chem. Phys. **208**, 233 (1996).
[17] A. Ricca and C. W. Bauschlicher, J. Chem. Phys. **106**, 2317 (1997).
[18] J. Niu, B. K. Rao, and P. Jena, J. Chem. Phys. **107**, 132 (1997).
[19] I. Boustani, Phys. Rev. B **55**, 16426 (1997).
[20] F. L. Gu, X. M. Yang, A. C. Tang, H. J. Jiao, and P. v. R. Schleyer, J. Comput. Chem. **19**, 203 (1998).
[21] I. Boustani and A. Quandt, Comput. Mater. Sci. **11**, 132 (1998).
[22] I. Boustani, A. Rubio, and J. A. Alonso, Chem. Phys. Lett. **311**, 21 (1999).
[23] M. L. McKee, Z. X. Wang, and P. v. R. Schleyer, J. Am. Chem. Soc. **122**, 4781 (2000).
[24] J. E. Fowler and J. M. Ugalde, J. Phys. Chem. A **104**, 397 (2000).
[25] J. Aihara, J. Phys. Chem. A **105**, 5486 (2001).
[26] P. Cao, W. Zhao, B. Li, B. Song, and X. Zhou, J. Phys.: Condens. Matter **13**, 5065 (2001).
[27] A. Petters, C. V. Alsenoy, N. H. March, D. J. Klein, and V. E. Van Doren, J. Phys. Chem. B **105**, 10546 (2001).
[28] W. Luo and P. Clancy, J. Appl. Phys. **89**, 1596 (2001).
[29] L. Hanley and S. L. Anderson, J. Phys. Chem. **91**, 5161 (1987).
[30] L. Hanley and S. L. Anderson, J. Chem. Phys. **89**, 2848 (1988).
[31] P. A. Hintz, S. A. Ruatta, and S. L. Anderson, J. Chem. Phys. **92**, 292 (1990).
[32] S. A. Ruatta, P. A. Hintz, and S. L. Anderson, J. Chem. Phys. **94**, 2833 (1991).

[33] P. A. Hintz, M. B. Sowa, S. A. Ruatta, and S. L. Anderson, J. Chem. Phys. **94**, 6446 (1991).
[34] S. J. La Placa, P. A. Roland, and J. J. Wynne, Chem. Phys. Lett. **190**, 163 (1992).
[35] M. B. Sowa-Resat, J. Smolanoff, A. Lapiki, and S. L. Anderson, J. Chem. Phys. **106**, 9511 (1997).
[36] A. I. Boldyrev and L. S. Wang, J. Phys. Chem. A **105**, 10759 (2001).
[37] L. S. Wang, H. S. Cheng, and J. Fan, J. Chem. Phys. **102**, 9480 (1995).
[38] L. S. Wang and H. Wu, in *Advances in Metal and Semiconductor Clusters. IV. Cluster Materials*, edited by M. A. Duncan (JAI, Greenwich, 1998), p. 299.
[39] L. S. Wang, J. Conceicao, C. Jin, and R. E. Smalley, Chem. Phys. Lett. **182**, 5 (1991).
[40] L. S. Wang and X. Li, in *Clusters and Nanostructure Interfaces*, edited by P. Jena, S. N. Khanna, and B. K. Rao (World Scientific, Englewood Cliffs, NJ, 2000) p. 293.
[41] X. Li, H. Wu, X. B. Wang, and L. S. Wang, Phys. Rev. Lett. **81**, 1909 (1998).
[42] J. Akola, M. Manninen, H. Hakkinen, U. Landman, X. Li, and L. S. Wang, Phys. Rev. B **60**, 11297 (1999).
[43] S. R. Liu, H. J. Zhai, and L. S. Wang, Phys. Rev. B **64**, 153402 (2001).
[44] A. D. McLean and G. S. Chandler, J. Chem. Phys. **72**, 5639 (1980).
[45] T. Clark, J. Chandrasekhar, G. W. Spitznagel, and P. v. R. Schleyer, J. Comput. Chem. **4**, 294 (1983).
[46] M. J. Frisch, J. A. Pople, and J. S. Binkley, J. Chem. Phys. **80**, 3265 (1984).
[47] R. G. Parr and W. Yang, *Density-Functional Theory of Atoms and Molecules* (Oxford University Press, Oxford, 1989).
[48] A. D. Becke, J. Chem. Phys. **98**, 5648 (1993).
[49] J. P. Perdew, J. A. Chevary, S. H. Vosko, K. A. Jackson, M. R. Pederson, D. J. Singh, and C. Fiolhais, Phys. Rev. B **46**, 6671 (1992).
[50] R. Krishnan, J. S. Binkley, R. Seeger, and J. A. Pople, J. Chem. Phys. **72**, 650 (1980).
[51] J. Cizek, Adv. Chem. Phys. **14**, 35 (1969).
[52] G. D. Purvis III and R. J. Bartlett, J. Chem. Phys. **76**, 1910 (1982).
[53] P. J. Knowles, C. Hampel, and H.-J. Werner, J. Chem. Phys. **99**, 5219 (1993).
[54] L. S. Cederbaum, J. Phys. B **8**, 290 (1975).
[55] W. von Niessen, J. Shirmer, and L. S. Cederbaum, Comput. Phys. Rep. **1**, 57 (1984).
[56] V. G. Zakrzewski and W. von Niessen, J. Comput. Chem. **14**, 13 (1993).
[57] V. G. Zakrzewski and J. V. Ortiz, Int. J. Quantum Chem. **53**, 583 (1995).
[58] For recent review see J. V. Ortiz, V. G. Zakrzewski, and O. Dolgunitcheva, in *Conceptual Trends in Quantum Chemistry*, edited by E. S. Kryachko (Kluver, Dordrecht, 1997), Vol. 3, p. 463.
[59] M. J. Frisch, G. M. Trucks, H. B. Schlegel *et al.*, Computer code GAUSSIAN 98 (revision A.7), Gaussian, Inc., Pittsburgh, PA, 1998.
[60] H.-J. Werner, P. J. Knowles, with contributions from R. D. Amos, A. Bernhardsson, A. Berning, Computer code MOLPRO-1999.
[61] G. Schaftenaar, Computer code MOLDEN 3.4, CAOS/CAMM Center, The Netherlands, 1998.
[62] X. Li, L. S. Wang, A. I. Boldyrev, and J. Simons, J. Am. Chem. Soc. **121**, 6033 (1999).
[63] G. D. Geske, A. I. Boldyrev, X. Li, and L. S. Wang, J. Chem. Phys. **113**, 5130 (2000).